

1 **Title: Towards phage therapy for acne vulgaris: Topical application in a mouse model**

2
3
4 **Authors:** Amit Rimon^{1,2,5}, Chani Rakov^{1,5}, Vanda Lerer¹, Sivan Sheffer-Levi³, Sivan
5 Alkalky-Oren¹, Tehila Shlomov⁴, Lihi Shasha¹, Ruthi Lubin¹, Shunit Copenhagen-
6 Glazer¹, Vered Molho-Pessach^{3,5}, Ronen Hazan^{1,5,6*}

7 **Affiliations:**

8 ¹Institute of Biomedical and Oral Research (IBOR), Faculty of Dental Medicine, Hebrew
9 University of Jerusalem; Jerusalem 91120, Israel

10 ²Tzameret, The Military Track of Medicine, Hebrew University-Hadassah Medical School,
11 Jerusalem 91120, Israel

12 ³Department of Dermatology, Hadassah Medical Center, Hebrew University of Jerusalem, The
13 Faculty of Medicine; Jerusalem 91120, Israel

14 ⁴Ophthalmology Department, Hadassah-Hebrew University Medical Center; Jerusalem 91120,
15 Israel.

16 ⁵These authors contributed equally

17 ⁶Lead contact

18 *Corresponding author: ronenh@ekmd.huji.ac.il

19 Keywords: Phage therapy, acne vulgaris, *Cutibacterium acnes*, antibiotic-resistance,
20 bacteriophage, topical therapy, neutrophile.

32 **SUMMARY**

33 Acne vulgaris is a common neutrophile-driven inflammatory skin disorder in which *Cutibacterium*
34 *acnes* (*C. acnes*) bacteria play a significant role. Until now, antibiotics have been widely used to
35 treat acne vulgaris, with the inevitable increase in bacterial antibiotic resistance. Phage therapy is
36 a promising solution to the rising problem of antibiotic-resistant bacteria, utilizing viruses that
37 specifically lyse bacteria.

38 Here, we explored the feasibility of phage therapy against *C. acnes*. By combining eight novel
39 phages we had isolated, together with commonly used antibiotics, we achieved 100% eradication
40 of clinically isolated *C. acnes* strains. Using topical phage therapy in an acne mouse model resulted
41 in significantly superior clinical scores, as well as a reduction in neutrophil infiltration compared
42 to the control group. These results demonstrate the potential of phage therapy in acne vulgaris
43 treatment, especially when antibiotic-resistant strains are involved.

44 45 46 **Main text**

47 **INTRODUCTION**

48 *Cutibacterium acnes* (*C. acnes*, previously termed *Propionibacterium acnes*) is a gram-positive,
49 lipophilic, anaerobic bacterium that is a skin microbiome resident (O'Neill and Gallo, 2018). *C.*
50 *acnes* plays a significant role in the pathogenesis of acne vulgaris, a common chronic inflammatory
51 disorder of the pilosebaceous unit (Dessinioti and Katsambas, 2010), affecting 80% of the
52 population during adolescence (Rzany and Kahl, 2006) as well as some adults (Zaenglein, 2018).
53 Although strains of *C. acnes* associated with healthy skin have been identified (phlotypes II and
54 III) (Lomholt and Kilian, 2010), other strains (phlotype IA) have been linked to acne (Lomholt
55 and Kilian, 2010).

56 The complex pathogenesis of acne involves androgen-mediated stimulation of sebaceous glands,
57 follicular hyperkeratinization, dysbiosis within the pilosebaceous microbiome, and innate and
58 cellular immune responses (O'Neill and Gallo, 2018).

59 *C. acnes* activates the innate immune response to produce proinflammatory interleukin (IL)-1 by
60 activating the nod-like receptor P3 (NLRP3) inflammasome in human sebocytes and monocytes
61 (Li et al., 2014). Moreover, *C. acnes* activates Toll-like receptor-2 in monocytes and triggers the
62 secretion of the proinflammatory cytokines IL-12 and IL-8. IL-8 attracts neutrophils and leads to

63 the release of lysosomal enzymes. These neutrophil-derived enzymes result in the rupture of the
64 follicular epithelium and further inflammation (Kim et al., 2002).

65 Acne has been treated for decades with topical and oral antibiotics, such as tetracycline (TET),
66 doxycycline (DOX), minocycline (MC), erythromycin (EM), and clindamycin (CM), aimed at *C.*
67 *acnes* (Muhammad and Rosen, 2013). Topical treatment modality is preferred when possible with
68 level A recommendation strength (Zaenglein et al., 2016), due to its local effect and lack of
69 systemic side effects (Zaenglein et al., 2016). However, an alarming global increase in antibiotic-
70 resistant *C. acnes* strains has occurred during the last two dozen years (Swanson, 2003). For
71 example, we (Sheffer-Levi et al., 2020) examined the sensitivity profile of 36 clinical isolates of
72 *C. acnes*, representing the verity of strains in Israel, to the abovementioned commonly used
73 antibiotics and found that the antibiotic resistance in this collection was 30.6% for at least one of
74 these antibiotics. These results correlate with the worldwide reported data of 20%–60% of resistant
75 strains (Karadag et al., 2020; Sheffer-Levi et al., 2020), indicating the need for other treatment
76 strategies aimed at *C. acnes*.

77 Bacteriophage (phage) therapy is evolving as one of the most promising solutions for emerging
78 antibiotic resistance. Phages are bacterial viruses widely distributed in the environment that
79 replicate within bacteria and specifically kill their bacterial targets without harming other flora
80 members. Therefore, they can be used as living drugs for various bacterial infections, including
81 acne (Jassim and Limoges, 2014).

82 The first *C. acnes* phage was isolated in 1964 by Brzin (BRZIN, 1964), but only in recent years
83 has phage therapy become a potential treatment approach for acne vulgaris, as reflected by the
84 increase in academic and industrial performance publications. Nevertheless, research on this topic
85 is lacking, as *in vivo* phage therapy in an acne mouse model has been tested only by intralesional
86 injections of *C. acnes* phages, and the efficacy of topical application, has not yet been shown (Kim
87 et al., 2019; Lam et al., 2021; Nelson et al., 2012).

88 Here, we present a direct topical application of *C. acnes* phages in an *in vivo* mouse model of acne
89 vulgaris as proof of the concept of phage therapy for acne. We tested our collection of *C. acnes*
90 strains for their *in vitro* susceptibility to eight novel phages we had isolated. Using an acne mouse
91 model, we then performed an *in vivo* evaluation of the efficacy and safety of topical application of
92 phages. To the best of our knowledge, this is the first demonstration of phage therapy for *C. acnes*
93 using a topical application.

94
95
96
97
98
99
100
101
102
103
104
105
106
107
108
109
110
111
112
113
114
115
116
117
118
119
120
121
122
123
124
125

RESULTS

Phage isolation

As part of the routine work of the Israeli Phage Bank (Yerushalmy et al., 2020), a screen for potential phages targeting *C. acnes* was performed. Eight phages targeting *C. acnes* were isolated from acne patients' saliva and Skin samples (Table 1). The phages were characterized as follows.

Genome sequencing and analysis

The genome of each phage was fully sequenced and analyzed (Figure 1, Table 1 and Supplemental table S1). All phages were similar, with a genome size range of 29,535–30,034 bp. Based on the absence of these phage sequences in bacterial genomes and the lack of typical lysogenic genes, such as repressors, integrases, or other hallmarks of lysogens, we assumed that they have a lytic lifecycle. The absence of repeat sequences indicates that their genomes have a linear topology. Phylogeny analysis showed that they belong to the Pahexavirus genera of the Siphoviridae family. BLAST alignment of the genomes revealed a high similarity between them and the genomes of many other published *Cutibacterium* phages from the Siphoviridae family.

Even though the phages were isolated separately, they showed a very high similarity of 87%–99%, with a coverage of 95%–98%. Phages PAVL33 and PAVL34 differed in a few point mutations and short insertions/deletions, mainly hypothetical or unrecognized phage proteins, and phylogenetically they seem to differ from all other phages (Figure 1, Table 1 and Supplemental table S1). As they were isolated from different samples, we considered them to be different. However, they could also be considered variants of the same strain.

The genome of the phages was found to be free from known harmful virulence factors or antibiotic resistance elements (data not shown), indicating that they were likely safe for phage therapy.

Phage visualization

The geometric structure and morphological characteristics of the *C. acnes* phages were visualized using transmission electron microscopy (TEM). As expected from their genome similarities, we did not observe any differences. They all had a similar capsid geometrical structure of an icosahedron, with a capsid diameter of 66 nm (Figure 2A), and a long noncontractile tail, with a length of 144 nm (Figure 2A).

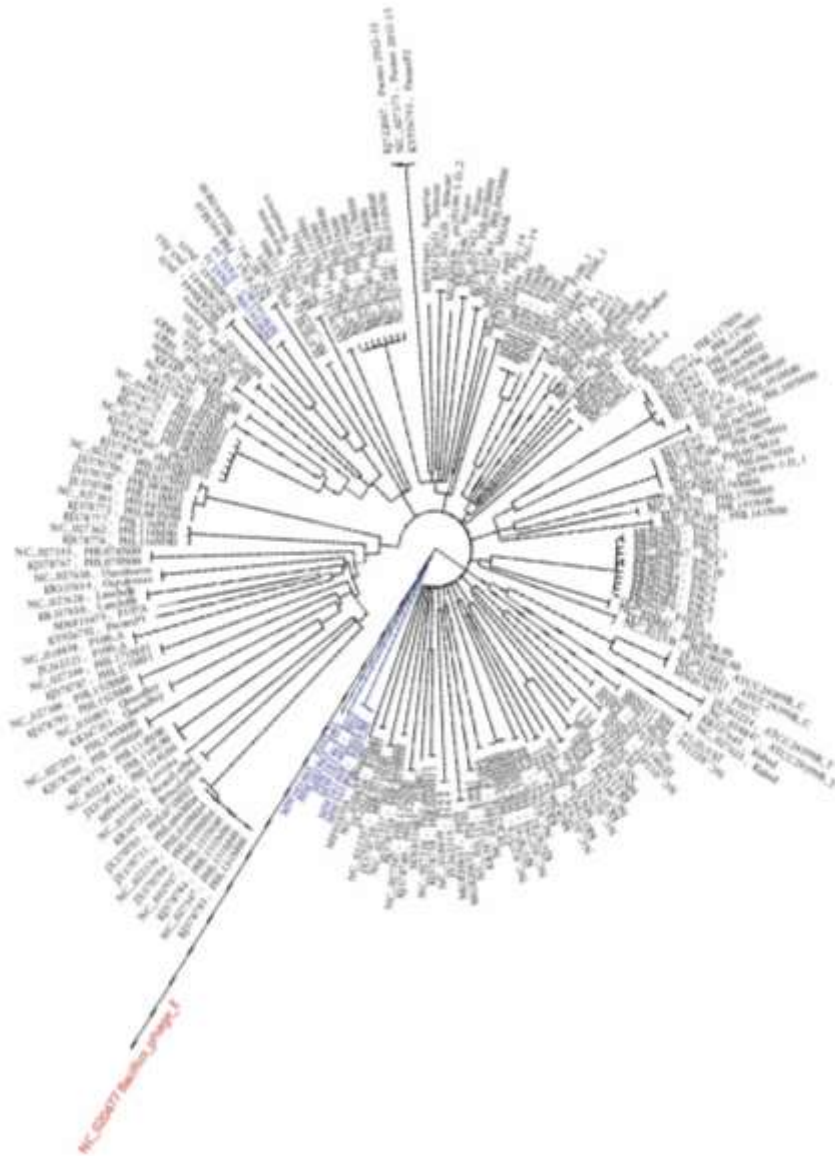
126

127 **Table 1. Characterization of eight novel *C. acnes* phages**

128

Phage	Origin of isolation	Genome Size (bp)	GC%	GenBank Accession
FD1	Saliva	29,774	54.3%	MW161461.1
FD2	Saliva	29,768	54.3%	MW161462.1
FD3	Saliva	29,638	54.2%	MW161463.1
PAVL20	Skin	29,800	54.3%	MW161464.1
PAVL21	Skin	30,034	54.3%	MW161465.1
PAVL45	Skin	29,772	54.3%	MW161468.1
PAVL33	Skin	29,627	54.4%	MW161466.1
PAVL34	Skin	29,535	54.3%	MW161467.1

129



130

131 **Figure 1. Phylogenetic tree**

132 novel isolated *C. acnes* targeting phages (blue) in comparison to all *C. acnes* targeting phages
133 found in blast (black). all results are relative to A *Bacillus* phage that is an out group. For more
134 details and accession numbers see Supplemental table S1.

135

136 **Host range coverage of phages *in vitro***

137 We tested the efficacy of the phages against *C. acnes* using solid media (agar plates) and liquid
138 cultures (Figure 2B–D and Supplemental Figure S2). Interestingly, despite the fact that the lysate
139 originated from a single plaque, we observed various sizes of clear plaques on the plates (Figure

140 2B). In the liquid culture, significant growth inhibition was observed with all phages (Figure 2C,
141 D) in the sensitive strains (Table 2). The CM-resistant strain 28 showed improved growth with
142 CM, but its growth was inhibited entirely by phage FD1 in the first 45 h of the experiment,
143 followed by regrowth afterward. Notably, the combination of phages and CM achieved complete
144 growth inhibition throughout the 65 h of the experiment (Figure 2C). Strain 21 showed the opposite
145 effect as it was resistant to the phages but sensitive to CM or to the combination of phage and CM
146 (Figure 2D). Thus, the combination provided 100% inhibition of all tested strains.

147
148 We tested the susceptibility profile of the *C. acnes* strains from our collection (8) to phages and
149 compared it to the previously tested susceptibility to various antibiotics (8). Of the 36 strains tested,
150 11 were resistant to at least one antibiotic (30.6%). We found that 32 of 36 *C. acnes* isolates (88%)
151 were phage susceptible. These 32 strains include all the above-mentioned strains resistant to at
152 least one antibiotic (34.4%), or resistant to all antibiotics (6.3%). Moreover, the four strains which
153 were phage-resistant were susceptible to all five tested antibiotics (Tables 2, Supplemental Table
154 S2, and Figure 2E).

155 **Table 2. Antibiotic and phage sensitivity of *C. acnes* strains.**

156 Erythromycin (EM), Clindamycin (CM), Tetracycline (TET), Doxycycline (DOX), and
 157 Minocycline (MC).

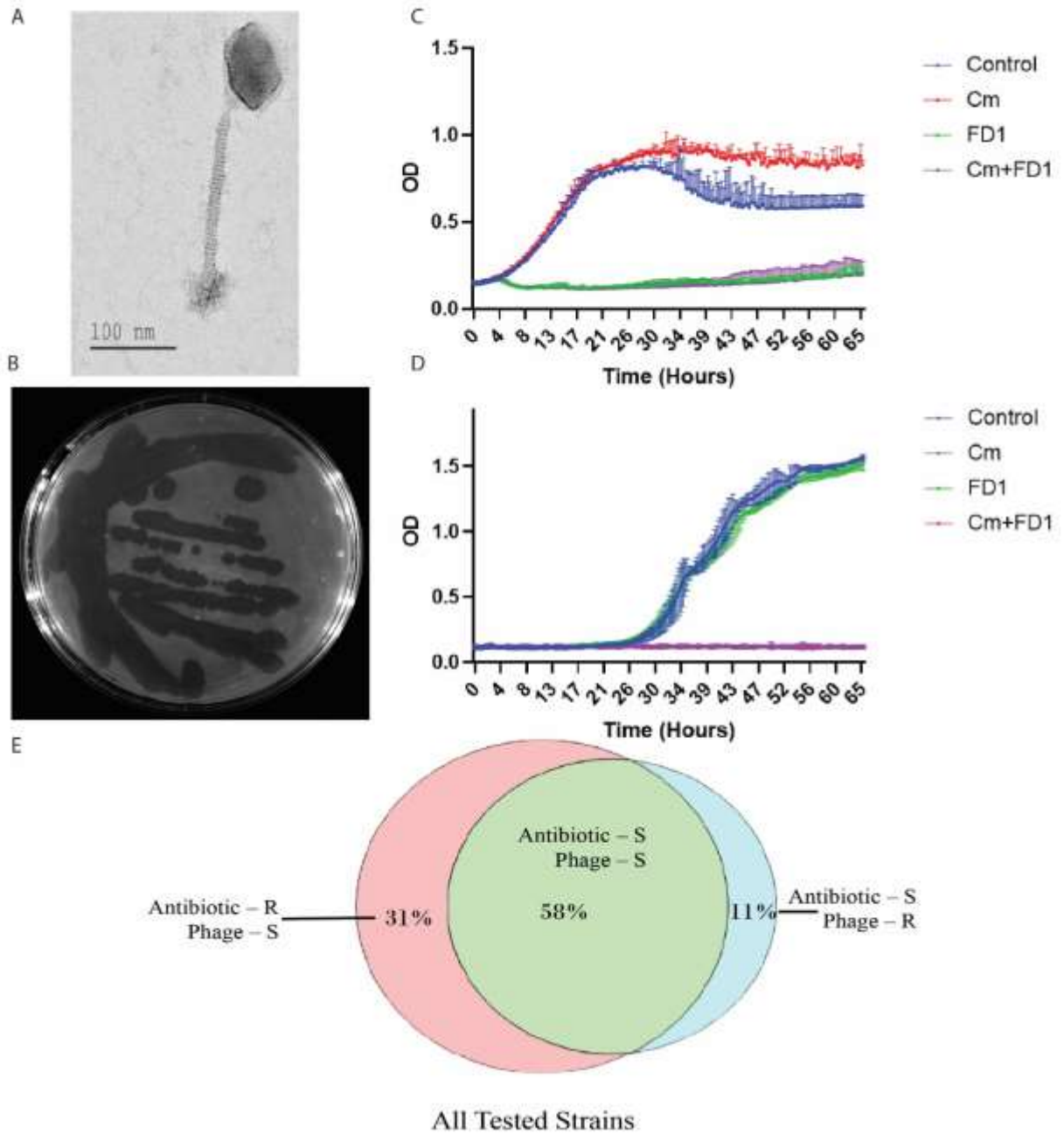
158 Strains were either sensitive (S), intermediate (I), or resistant (R) to antibiotics. All strains were
 159 either sensitive (S) or resistant (R) to all eight phages tested in the phage column (P).

#	P	EM	EM+P	CM	CM + P	TET	TET+P	DOX	DOX + P	MC	MC+P	All AB	All AB+P
1	S	S	S	S	S	S	S	S	S	S	S	S	S
2	S	R	S	R	S	I	S	R	S	I	S	S	S
4	R	S	S	S	S	S	S	S	S	S	S	S	S
5	S	R	S	R	S	R	S	R	S	S	S	S	S
6	S	S	S	S	S	S	S	S	S	S	S	S	S
7	S	R	S	I	S	I	S	I	S	S	S	S	S
8	S	S	S	S	S	S	S	S	S	S	S	S	S
9	S	S	S	S	S	S	S	S	S	S	S	S	S
10	S	S	S	S	S	S	S	S	S	R	S	S	S
11	S	S	S	S	S	S	S	S	S	S	S	S	S
13	S	S	S	S	S	I	S	S	S	S	S	S	S
14	S	R	S	R	S	R	S	R	S	R	S	R	S
15	S	S	S	S	S	S	S	S	S	S	S	S	S
18	S	S	S	S	S	S	S	S	S	S	S	S	S
19	S	S	S	S	S	S	S	I	S	S	S	S	S
21	R	S	S	S	S	S	S	S	S	S	S	S	S
22	S	S	S	S	S	S	S	S	S	S	S	S	S
23	S	S	S	S	S	S	S	S	S	R	S	S	S
24	S	R	S	I	S	S	S	S	S	S	S	S	S
25	S	R	S	I	S	I	S	R	S	I	S	I	S
27	S	S	S	S	S	S	S	S	S	S	S	S	S
28	S	R	S	R	S	I	S	R	S	S	S	S	S
30	S	S	S	S	S	S	S	S	S	S	S	S	S
31	S	R	S	R	S	I	S	R	S	I	S	I	S
32	S	S	S	S	S	S	S	S	S	S	S	S	S
33	R	S	S	S	S	S	S	S	S	S	S	S	S
35	S	R	S	R	S	R	S	R	S	R	S	R	S
36	S	S	S	S	S	S	S	S	S	S	S	S	S
37	S	S	S	S	S	S	S	S	S	S	S	S	S
40	S	S	S	S	S	S	S	S	S	S	S	S	S
41	S	S	S	S	S	S	S	S	S	S	S	S	S
43	S	S	S	S	S	S	S	S	S	S	S	S	S
44	S	S	S	S	S	S	S	S	S	S	S	S	S
47	S	S	S	S	S	S	S	S	S	S	S	S	S
48	R	S	S	S	S	S	S	S	S	S	S	S	S
49	S	S	S	S	S	S	S	S	S	S	S	S	S

160

161

162



163

164

165 **Figure 2. *In vitro* phage activity and coverage.**

166 (A) Transmission electron microscopy of FD1 phage.

167 FD1 plaques on strain 27. Note the various sizes of plaques, despite the fact that they
168 originated from a single plaque, and no lysogen was detected when the lytic phage was
169 sequenced.

170 (B) CM-resistant strain 28, growth with CM, FD1 phage, and their combination. The results
171 are the average of triplicates, presented as mean \pm SD.

172 (C) FD1-resistant strain 21 growth with CM, FD1 phage, and their combination. Note that the
173 two lower curves, CM and CM + FD1, overlap. The results are the average of triplicates,
174 presented as mean \pm SD.

175 (E) Venn diagram of the phage and antibiotic susceptibility, S – susceptible to all tested
176 antibiotics or phages, R – resistant.

177

178 **Acne mouse model of phage therapy *in vivo***

179 We assessed the potential of phages for *C. acnes* infection using our isolated phages. To this end,
180 we infected mice with *C. acnes* strain 27, a clinical isolate from a patient with severe acne vulgaris.
181 We used FD3 as the representative phage, which showed high *in vitro* efficacy against strain 27
182 (Figure 2B) and was stable for a week in carbopol gel preparation (2.5%) at room temperature and
183 at 4°C without any significant reduction of its titer (data not shown).

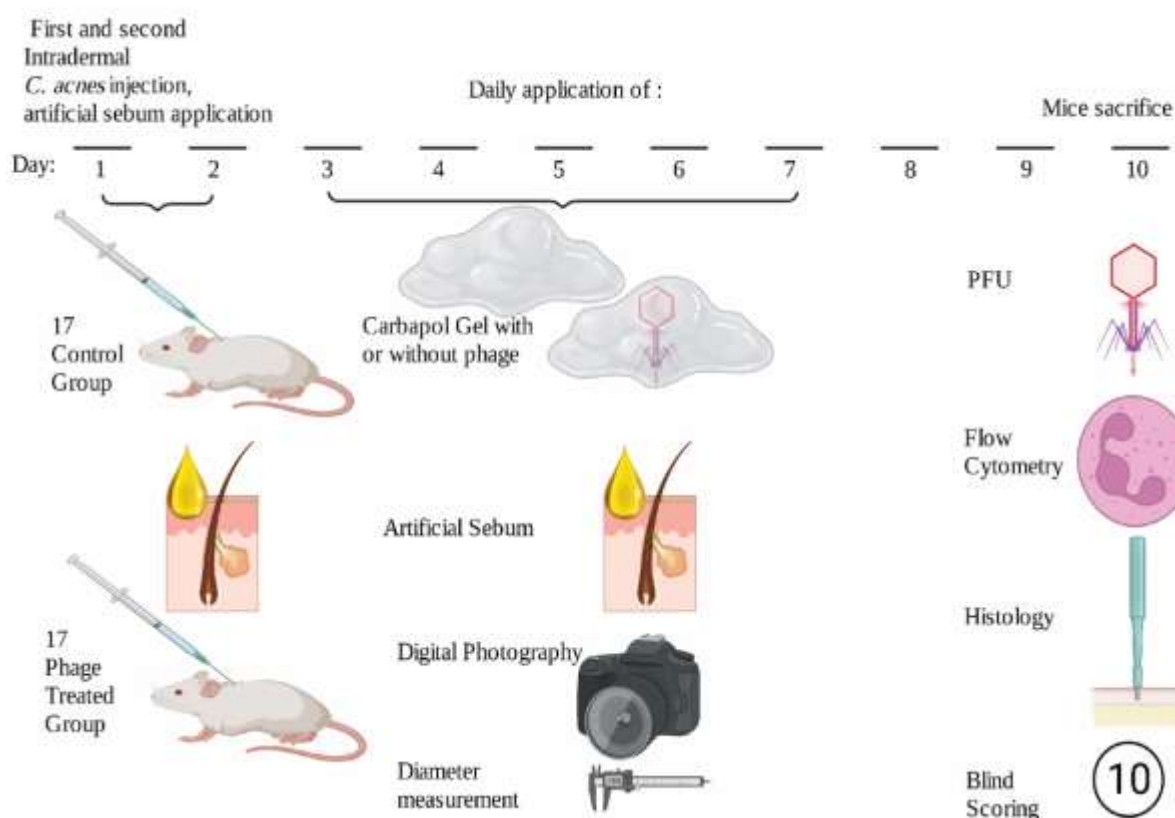
184 The infection was carried out by two intradermal injections of strain 27 on two consecutive days
185 to the back of 34 Balb/c (ICR) mice (days one and two, respectively), followed by daily topical
186 application of artificial human sebum (Kolar et al., 2019) to the injection site. This treatment
187 yielded significant inflammatory acne lesions at the injection site by day 3 (Figure 3). Once
188 inflammatory lesions were established, the mice were randomized into two groups of 17 mice
189 each. One group was treated with FD3 phage in carbopol gel applied daily for five consecutive
190 days, and the other group was treated with carbopol gel only. Photographs of the lesions were
191 taken, and the lesions' diameter, elevation/papulation of lesions, and the presence of eschar over
192 lesions were assessed daily. A clinical score was defined to assess the severity of inflammatory
193 lesions based on a modified revised acne Leeds grading system (O'brien et al., 1998) and other
194 methods previously described for acne vulgaris (Agnew et al., 2016; Qin et al., 2015). Mice were
195 sacrificed and biopsies were taken on day 10. Biopsies underwent histopathological assessment,
196 and were analyzed for the presence of bacteria and phages at the lesion site by polymerase chain
197 reaction (PCR), colony-forming unit (CFU), and plaque-forming unit (PFU) determination in a

198 homogenized tissue biopsy, respectively. For more details, refer to the Assessment of Phage
199 Clinical Efficacy section in Materials and Methods and Figure 7.

200 The plaques of FD3 were isolated from a skin biopsy taken on day 10, three days after the last
201 administration of the 2.5% phage-containing carbopol gel.

202 Mice treated with phage and mice treated with vehicle did not develop any adverse events during
203 this experiment. The daily application of FD3 for five consecutive days resulted in improvement
204 in three clinical parameters (diameter of inflammatory lesions, papulation/elevation of lesions, and
205 presence and severity of eschar over lesions) compared to mice treated with vehicle only (Figure
206 4A - F and Supplemental Table S3).

207



208

209 **Figure 3. Schematic description of phage therapy *in vivo* in an acne mouse model.**

210 Mice were injected intradermally on days one and two. Throughout days 3–7, mice were treated
211 with topical carbopol gel for the control group and phage-containing carbopol gel for the phage-
212 treated group. Artificial sebum was applied daily starting from day 1. Mice were sacrificed on
213 day 10 and analyzed as described (This Figureure was made with biorender.com)

214

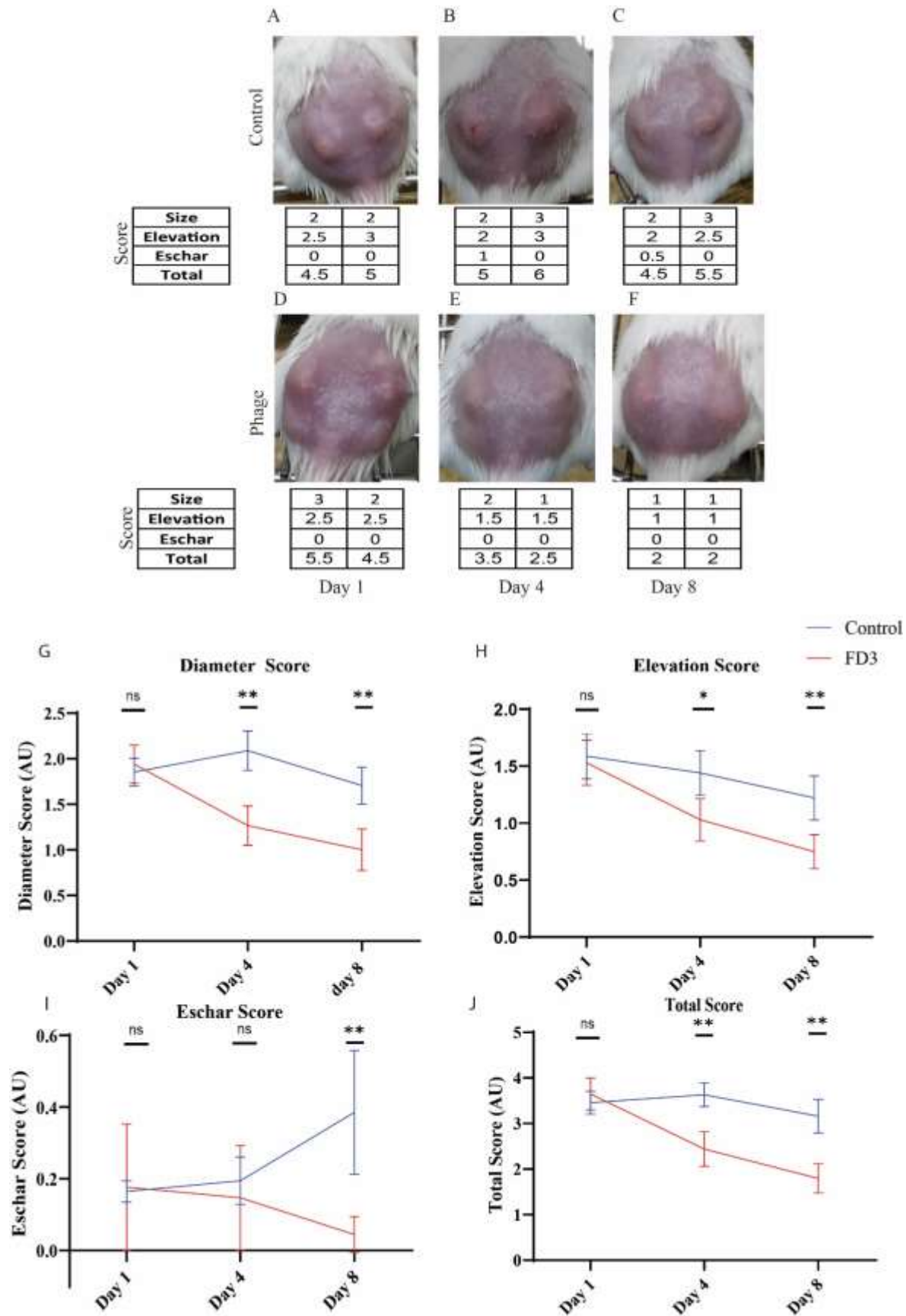
215 The differences in the lesion diameters were significant starting from day four, with a score of 2.09
216 arbitrary units (AU) (5.2 mm) in the control group versus 1.27 (3.6 mm) in the treated group (p-
217 value < 0.001, Figure 4G). The phage-treated group showed a continuous reduction in the lesion
218 diameter, from an average score of 1.93 AU (4.6 mm on day one) to 1.00 AU (2.9 mm on day
219 eight) (p-value < 0.001, Figure 4G). Conversely, the control group's average lesion diameter
220 changed in a non-continuous manner, increasing from an average score of 1.82 (4.5 mm on day
221 one) to 2.09 AU (5.2 mm on day four) in the early days of the experiment, followed by a decrease
222 to 1.7 AU (4.5 mm on day eight) at the end of the experiment (Figure 4G). A spontaneous reduction
223 was observed in the control group toward the end of the experiment (Figure 4G).

224 Another clinical parameter assessed was the degree of elevation (papulation) of the inflammatory
225 lesions (Figure 7). Significant differences were observed between the treated and control groups
226 on the latter days of the experiment. The lesions' average elevation score on day zero was 1.57
227 AU (average of 34 lesions) in control group and 1.52 AU in phage-treated group (non-significant).
228 However, it decreased to 0.75 AU in the treated group and was 1.2 AU on day 8 in the control
229 group (p-value < 0.001, Figure 4H).

230 The third clinical parameter was the presence of eschar in the inflammatory lesions (Figure 7). The
231 number and severity of eschar in mice increased significantly in the control group, whereas the
232 average eschar score in the phage-treated mice was lower (p-value < 0.01, Figure 4I). The
233 comparison of the combined scores of the three clinical parameters between the two groups (Figure
234 7) was significant on days 4–8 (p-value < 0.001 at both timepoints, Figure 4J).

235

236



238 **Figure 4.**

239 **Clinical scoring of inflammatory lesions. Mice # 11 (from the control group) and mice # 12**
240 **(from the treated group) are shown as representative examples.**

241 (A-C) Photographs taken on days one, four, and eight and the clinical scores are presented. The
242 diameter of the lesions, degree of elevation (papulation), and presence and severity of eschar
243 were evaluated using a scoring system. For more details, refer to the Materials and Methods
244 section. Control mice lesions. (D-F) phage-treated mice lesions.

245 (G-J) The scores of the diameter, degree of elevation, eschar, and combined scores are shown
246 accordingly, in blue (control group) and red (phage group) at three timepoints. Data is presented
247 as mean \pm SD.

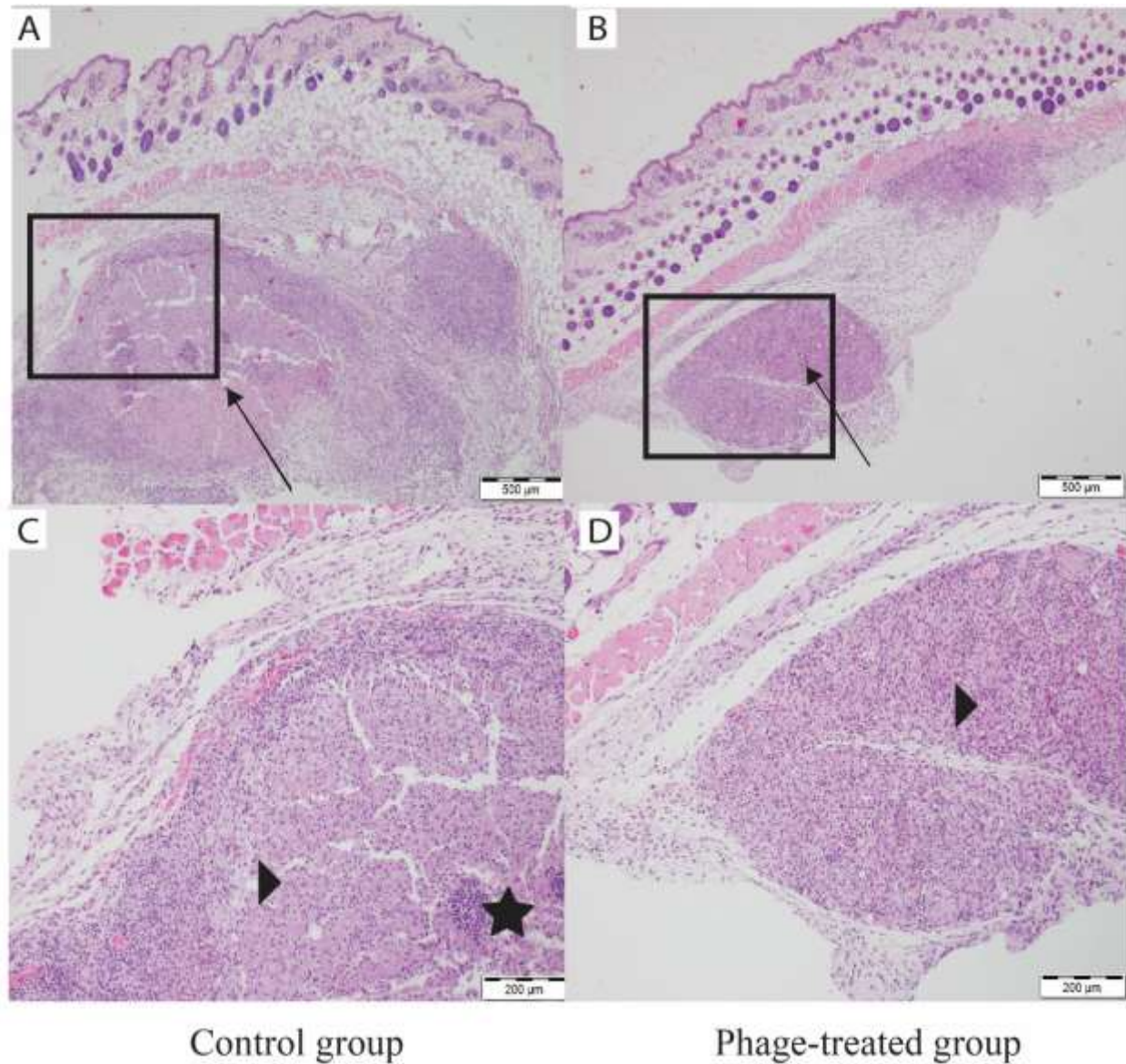
248 Student's *t-test* two-tailed unpaired p-values between the control group and the FD3-treated
249 group. *p-value < 0.05, **p-value < 0.001. Eschar score is corrected to the same value at day 1.
250 For details on all mice see Supplemental Table S3.

251

252 **Histopathological evaluation of inflammatory lesions**

253 Histopathological evaluation was performed on the biopsies taken from both groups' inflammatory
254 lesions on day eight of the experiment (Figure 5).

255 The skin of the control mice showed evidence of a more severe and acute pyogranulomatous
256 inflammatory process. In some cases, the inflammation involved the dermis and subcutaneous
257 tissue (Figure 5A). A nodular infiltrate, with an area of necrosis with small numbers of interspersed
258 neutrophils surrounded by macrophages and rare lymphocytes, was observed (Figure 5C). By
259 contrast, inflammation was less severe in the phage-treated group, with mostly chronic
260 granulomatous infiltration, involving only subcutaneous tissue below the panniculus carnosus
261 mixed with minimal numbers of neutrophils (Figure 5B, D).



262

Control group

Phage-treated group

263 **5. Histology of inflammatory lesions.**

264 (A) Nodular inflammation (arrow) involving the dermis and subcutaneous tissue at 4×
265 magnification in the control group.

266 (B) nodular inflammation (arrow) involving only the subcutaneous tissue below the panniculus
267 carnosus at 4× magnification in the phage-treated group.

268 (C) A nodular infiltrate with an area of necrosis with small numbers of interspersed neutrophils
269 (stars) surrounded by macrophages (arrowhead) and rare lymphocytes at 10× magnification in the
270 control group.

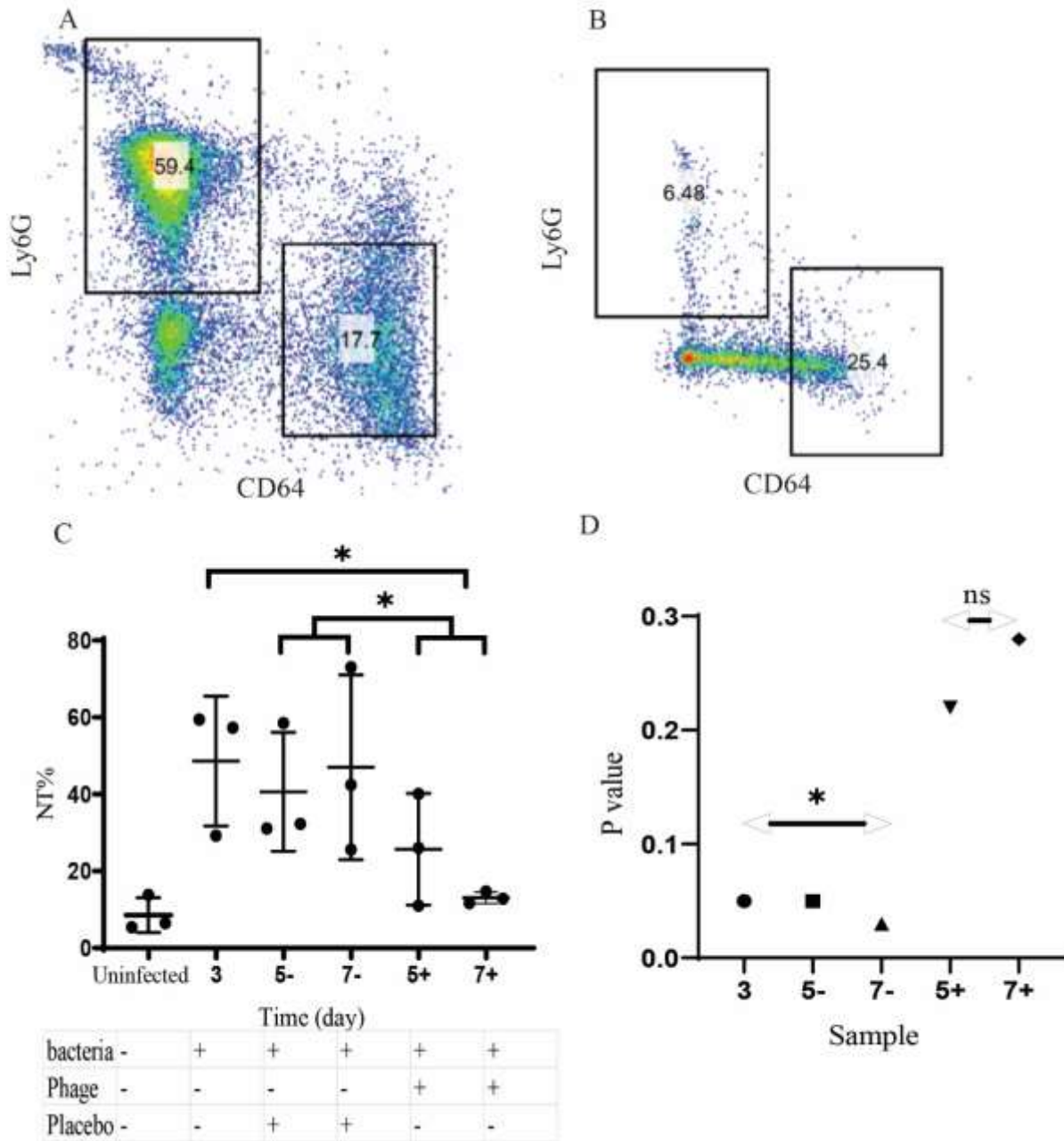
271 (D) A nodular infiltrate of macrophages (arrowhead), many with vacuolated cytoplasm mixed with
272 a minimal number of neutrophils at 10× magnification in the phage-treated group.

273

274

275 **Evaluation of neutrophilic inflammatory reaction**

276 Three mice were sacrificed at different time points: day three (after establishing inflammatory
277 lesions, before commencing treatment with carbopol or phage), day five, and day seven of the
278 treatment with carbopol alone or phage. Three uninfected mice were sacrificed as the negative
279 control (uninfected). Skin specimens underwent evaluation by flow cytometry (Materials and
280 Methods). Antibodies for Ly6G, CD64, CD11b, and CD45 were used to identify different cell
281 populations. As acne is a neutrophil-driven process, we decided to specifically examine the
282 neutrophilic infiltrate in the specimens collected using the neutrophilic marker Ly6G+ (Swamydas
283 et al., 2015). On day three, the average neutrophil percentage (%NT) was 48.63% in *C. acnes*-
284 injected mice (see a representative example in Figure 6A). The skin specimen of the control
285 uninfected mice had 11.21%NT (See representative example in Figure 6B,). On day five, the
286 average %NT was 40.6% in the infected untreated control group and 25.12% in the infected phage-
287 treated group. On day seven of the experiment, the average %NT was 35.22% in the infected
288 untreated control group and 17.6% in the infected phage-treated group. Bacteria-injected mice on
289 day three, before the group allocation were significantly different from the phage-treated group on
290 day seven (p-value = 0.02), and the placebo-treated group was different from the phage-treated
291 group (p-value = 0.02) (Figure 6C). The lesions of phage-treated mice had normalized to the
292 uninfected control on days five and seven (p-value = 0.22, 0.28 accordingly), whereas the control-
293 treated group did not normalize (p-value < 0.05) (Figure 6D).
294 Monocytes were also examined (CD64+) (Genel et al., 2012), without significant dynamics in this
295 model.



296

297 **Figure 6. Flow cytometry at various timepoints.**

298 (A) *C. acnes* infected mice on day three of the experiment, 59% of the myeloid cells (%NT) (CD64
299 Negative, Ly6 G positive).

300 (B) uninfected control, 6%NT.

301 (C) Flow cytometry analysis. A significant difference was found between day three and day seven
302 in the phage group and between the phage group and the control group. Data is presented as mean
303 \pm SD.

304 (D) The p-value of each group compared to the uninfected group.

305 The Mann–Whitney U test was used. * denotes p-value < 0.05 and **ns** “not significant”.

306

307 **DISCUSSION**

308

309 This study presents a phage-based topical treatment in an acne mouse model. The results provide
310 *in vivo* support for the efficacy and safety of transdermal phage therapy in treating acne vulgaris
311 and shed light on the cytological modification involved in the response to phage therapy.

312 Antibiotic resistance of *C. acnes* has been reported worldwide. Regional differences and dynamic
313 changes over time are remarkable, and an increase in resistance rates has been reported (Coates et
314 al., 2002; Karadag et al., 2020; Sheffer-Levi et al., 2020). Studies on phage susceptibility have
315 also been performed (Brüggemann and Lood, 2013; Castillo et al., 2019; Jong et al., 1975; Liu et
316 al., 2015; Marinelli et al., 2012), demonstrating an average of 88% susceptibility to *C. acnes*,
317 consistent with our findings of an 88.8% susceptibility rate (Brüggemann and Lood, 2013; Castillo
318 et al., 2019).

319 Nevertheless, to the best of our knowledge, the current study is the first to demonstrate full
320 treatment coverage of *C. acnes* strains using a combination of antibiotics and phages (Figure 2E).
321 As previously shown on *Acinetobacter baumannii* (28), this may indicate that resistance to one
322 modality of treatment interferes with resistance to the other. Further research is needed to clarify
323 whether resistance mechanisms induce the re-sensitization of the other.

324 Among the *C. acnes* strains resistant to a given antibiotic, the phage–antibiotic combination caused
325 effective inhibition, indicating that phage therapy could serve as an optional treatment for
326 antibiotic-resistant acne. In all investigated strains, whether they were resistant to a specific
327 antibiotic or phage, a combination of phage and antibiotic showed a non-inferior response to
328 treatment with antibiotics alone. This shows that a combination of phages and any given antibiotic
329 may be an effective empiric regimen (Figure 2, Table 2) (Katsambas et al., 2004; Zaenglein et al.,
330 2016).

331 Therefore, we suggest that phage therapy should be evaluated for the treatment of acne vulgaris,
332 especially in antibiotic-resistant cases, perhaps in combination with conventional therapy. This
333 approach may give superior results *in vivo* and lead to a decrease in the development of antibiotic-
334 resistant strains. *In vivo* and clinical data are needed to confirm this assumption.

335 *C. acnes* strains showed an “all or none” susceptibility to all phages; bacterial strains that were
336 resistant to a single phage, with no exceptions, showed resistance to all eight phages. Bacteria that
337 showed susceptibility to one phage showed susceptibility to all phages (Table 2 and Supplemental
338 Table S2).

339 *C. acnes* phages are known to demonstrate small variability, to which most isolated *C. acnes* strains
340 are susceptible, with little genomic variance (Castillo et al., 2019; Marinelli et al., 2012). The two
341 possible theories explaining the small variety are as follows: 1) small niche theory: the fact that
342 the life niche of *C. acnes* is only in the pilosebaceous unit makes it difficult for phages to go
343 through different varieties of bacteria (Castillo et al., 2019); 2) bottleneck theory: evolutionary
344 limitations have made it possible for only one family of phages to survive (Castillo et al., 2019).
345 Phage isolation from saliva reflects the presence of *C. acnes* phages and bacteria in this
346 environment, tipping the scale away from the “small niche theory.” The isolated phages show
347 limited evolutionary space and are all part of the same phylotype (Abedon, 2009). One possible
348 theory of an evolutionary force involves prokaryotic innate immunity in the form of repeating
349 palindromic nucleotides that correlate with resistance to several phages (Marinelli et al., 2012).
350 For example, unlike *C. acnes* phages, *Propionibacterium freudenreichii* phages are more diverse
351 (Cheng et al., 2018). Perhaps the evolutionary forces differ between species. The latter is not part
352 of the human microbiome and is an important part of the cheese manufacturing process and a
353 possible probiotic (Thierry et al., 2011).

354 Moreover, the high genomic similarity of our *C. acnes* phages, together with the high similarity
355 observed in other known *C. acnes* phages, shows that a more precise taxonomic method is required
356 to determine whether the given phage is new. One option is to compare only the specific gene/s
357 and not entire genomes.

358 Previous studies have assessed the activity and efficacy of injected acne phages in an acne mouse
359 model (Kim et al., 2019; Lam et al., 2021; Nelson et al., 2012). Such a method of phage delivery
360 is not clinically applicable. Our work is the first *in vivo* demonstration of the efficacy and safety
361 of topically applied phages in an acne mouse model, providing further support for the potential
362 role of phage therapy in acne vulgaris.

363
364

365 The establishment of an acne mouse model is not trivial, as acne is solely a human disease (Plewig
366 et al., 2019). The use of artificial sebum and two consecutive injections of a clinically isolated *C.*
367 *acnes* strain enabled us to induce inflammatory lesions, simulating inflammatory papules and
368 nodules of acne vulgaris (Figure 4 and Supplemental Table S3). Our model showed a self-resolving
369 effect, with spontaneous recovery of the inflammatory lesions over time (Figure 4 and
370 Supplemental Table S3). Therefore, the treatment period was limited to five days, whereas any
371 treatment for acne vulgaris in humans, including antibiotics, was given for weeks and months
372 (Zaenglein et al., 2016). Despite the concise treatment period provided in our acne mouse model,
373 we observed significant and fast improvement in the inflammatory lesions in the FD3-treated
374 group compared to the control group (Figures. 4-6).

375 The significant earlier and faster clinical improvement in the FD3-treated group suggests a positive
376 effect of FD3, which is further supported by evidence of reduced neutrophilic infiltration, both in
377 histopathology, and flow cytometry analysis. Neutrophil-mediated inflammation is an essential
378 part of acne vulgaris pathogenesis. The described reduced percentage of neutrophils in the lesions
379 could be due to fewer bacteria in the tissue. Another possible mechanism is phage–innate immunity
380 interactions, which have been described mainly *in vitro* (Van Belleghem et al., 2019) (Figures. 5,
381 6). Further testing of immunological *in vivo* data is needed to assess this hypothesis. Based on our
382 results, early in the course of the inflammatory lesions, there seemed to be a dominant neutrophilic
383 infiltration, but phage therapy induced faster neutrophilic clearance or inhibited neutrophilic
384 migration later in the course of the lesions. Moreover, bacterial infected phage-treated mice were
385 not significantly different from the uninfected control skin, whereas the bacterial infected untreated
386 control mice were significantly different from the negative control.

387
388 Although one of our aims was to show the efficacy of topical application of the phage, we were
389 concerned that the phage might not penetrate the skin. However, we were able to show phage
390 penetration by isolating the phages from the lesions three days post-administration. Therefore, we
391 assume that phages penetrate the lesion and multiply inside it, using the target bacterium.

392 In this study we did not examine the efficacy of a combination of phages and antibiotics in our
393 mouse model. The isolated strain used in this model was not antibiotic resistant, and we focused
394 on investigating phage efficacy alone. Phages that have been proven efficient should be assessed
395 for synergism with antibiotics in another mouse model and in clinical trials.

396

397

398 According to the collected data and in light of the harmless expected effect of phages on the skin
399 microbiome (Barnard et al., 2016), we hypothesize that phage therapy is a promising treatment
400 modality for acne vulgaris. Nevertheless, this should be further tested in clinical trials. If anti-*C.*
401 *acnes* phage treatment is found to be safe and effective in humans, it is expected to be used in the
402 future to treat acne vulgaris and reduce the widespread use of antibiotics in this common skin
403 condition.

404

405 **MATERIALS AND METHODS**

406

407 **Bacterial clinical isolates**

408 This study used a collection of 36 *C. acnes* clinical isolates with various ribotype single-locus
409 sequence typing (SLST) types (Figure S1) obtained from the Department of Clinical Microbiology
410 and Infectious Diseases of Hadassah Medical Center, as we previously described (Sheffer-Levi et
411 al., 2020). Unless mentioned otherwise, the *C. acnes* isolates were grown in Wilkins–Chalgren
412 broth (Difco, Sparks, MD, USA) at 37°C under anaerobic conditions and stored at –80°C in
413 glycerol (25%) until use. Bacterial concentrations were evaluated using 10 µl of 10-fold serial
414 dilutions plated on Wilkins agar plates under anaerobic conditions. Colonies were counted after 48
415 h at 37°C, and the number of CFU/mL was calculated.

416

417 **Antibiotic susceptibility**

418 Following bacterial identification, *C. acnes* isolates were sub-cultured in Wilkins broth (Oxoid,
419 Basingstoke, UK) and suspended at a density of 1.0 McFarland. Bacterial lawns were prepared on
420 anaerobic blood plates (Novamed, Jerusalem, Israel) and dried. Antibiotic susceptibility was
421 assessed by determining a minimal inhibitory concentration (MIC) using an epsilometer test
422 (ETEST® bioMérieux, St. Louis, MO, USA). The MIC was determined following 48 h of
423 incubation under anaerobic conditions as the point on the scale at which the ellipse of growth
424 inhibition intercepts the plastic strip. The antibiotics used tetracycline (TET), doxycycline (DOX),
425 minocycline (MC), erythromycin (EM), and clindamycin (CM),. The breakpoints used to define
426 susceptibility or resistance to CM and TET followed the recommendations set by the Clinical and

427 Laboratory Standards Institute (Wayne, 2017). Resistance to CM was defined at an MIC above 2
428 $\mu\text{g/ml}$ and to TET at an MIC above 4 $\mu\text{g/ml}$. As no standards exist for the breakpoints of EM,
429 DOX, and MC, those with an MIC of $\geq 0.5 \mu\text{g/ml}$ (for EM) and $\geq 1 \mu\text{g/ml}$ (for DOX and MC)
430 were defined as resistant according to the definitions used in previous studies (Toyne et al., 2012).
431 CM (1.5 $\mu\text{g/ml}$) and EM (15 $\mu\text{g/ml}$) were the antibiotics used when assessing phage antibiotic
432 synergism.

433

434 **Phage isolation and propagation**

435 The phages were isolated using the standard double-layered agar method, as previously described
436 (Adams, 1959). Briefly, 1–5 ml of saliva or skin samples were mixed with 5 ml of phage buffer
437 (150 mM NaCl, 40 mM Tris-Cl, pH 7.4, 10 mM MgSO_4) centrifuged on the following day
438 (centrifuge 5430R, rotor FA-45-24-11HS; Eppendorf, Hamburg, Germany) at 10,000 g for 10 min.
439 The supernatant was filtered first through filters with a 0.45- μm pore size (Merck Millipore, Ltd.,
440 Ireland) and then through filters with a 0.22- μm pore size (Merck Millipore Ltd., Ireland).
441 Exponentially grown bacterial cultures were inoculated with filtered skin or saliva effluent for 24
442 h at 37°C in an anaerobic jar. The cultures were filtered again and added to 5 ml of Wilkins–
443 Chalgren agar (Oxoid Basingstoke, United Kingdom) containing 0.5 ml of overnight-grown *C.*
444 *acnes* after centrifugation. The supernatant was filtered as described and plated using soft agar
445 (0.6%) overlaid with the test strain and then incubated overnight at 37°C in an anaerobic jar, as
446 described above. Clear plaques were observed and transferred into a broth tube using a sterile
447 Pasteur pipette. The phage stocks were inoculated with bacterial cultures to collect high titer
448 lysates, which were then stored in Wilkins at 4°C.

449

450 **Determination of phage concentration**

451 The phage solution was inoculated into 5 ml of pre-warmed Wilkins soft agar (0.6%). A 0.1 ml
452 portion of an overnight culture of *C. acnes* was added to the tube and placed on a Wilkins agar
453 plate. The plates were incubated anaerobically for 48 h, and the appearance of plaques on the plates
454 was used to determine whether the bacteria were phage-susceptible. The phage concentration was
455 determined according to the standard PFU method. Lysates were serially diluted 10-fold into 5 ml
456 of pre-warmed Wilkins soft agar (0.6%). A 0.1 ml portion of an overnight culture of *C. acnes* was
457 added to the tube, placed on a Wilkins agar plate, and grown anaerobically for 48 h. The number

458 of plaques was counted, and the initial concentration of PFU/mL was calculated (Adams, 1959).
459 If not specified otherwise, phages were grown to an initial concentration of 10^8 PFU/ml.

460 **Growth kinetics**

461 Logarithmic (10^7 CFU/ml) *C. acnes* cultures with phages and antibiotic concentrations, as
462 described, were put in a total volume of 200 μ l in triplicates. The growth kinetics of the cultures
463 were recorded at 37°C anaerobic conditions sealing the contents of an anaerobic bag (Thermo
464 Fisher Scientific, Waltham MA, USA) on the outer cells of a 96 well plate, with 5 s shaking every
465 20 min in a 96-well plate reader (Synergy; BioTek, Winooski, VT) at 600 nm. The mean and 95%
466 confidence intervals are shown.

467

468 **Genome sequencing and analysis**

469 The DNA of the phages was extracted using a phage DNA isolation kit (Norgen Biotek, Thorold,
470 Canada) (Summer, 2009). Libraries were prepared using an Illumina Nextera XT DNA kit (San
471 Diego, CA, USA). Normalization, pooling, and tagging were performed using a flow cell with $1 \times$
472 150 bp paired-end reads, which were used for sequencing with the Illumina NextSeq 500 platform.
473 Sequencing was performed in the sequencing unit of the Hebrew University of Jerusalem at the
474 Hadassah Campus. Trimming, quality control, reads assembly, and analyses were performed using
475 Geneious Prime 2021.2.2 and its plugins (<https://www.geneious.com>). Assembly was performed
476 using the SPAdes plugin of Geneious Prime. Annotation was performed using RAST version 2
477 (<https://rast.nmpdr.org/rast.cgi>, accessed on March 1, 2021), PHAge Search Tool Enhanced
478 Release (PHASTER) (<https://phaster.ca>, accessed on March 1, 2021), and the BLAST server. The
479 phages were scanned for resistance genes and virulence factors using ABRicate (Seemann T,
480 ABRicate, <https://github.com/tseemann/abricate>) based on several databases: NCBI, CARD,
481 Resfinder, ARG-ANNOT, EcoOH, MEGARES, PlasmidFinder, Ecoli_VF, and VFDB.

482 **TEM**

483 A lysate sample (1 ml) with 10^8 PFU/ml was centrifuged at 20,000 g (centrifuge 5430R, rotor
484 FA-45-24-11HS; Eppendorf, Hamburg Germany) for 2 h at room temperature. The supernatant
485 was discarded, and the pellet was resuspended in 200 μ l of 5 Mm MgSO₄. This sample was spotted
486 on a carbon-coated copper grid, with an addition of 2% uranyl acetate and incubated for 1 min; the
487 excess was removed (Yazdi et al., 2020). The sample was visualized using a transmission electron
488 microscope (TEM 1400 plus Joel, Tokyo, Japan), and a charge-coupled device camera (Gatan

489 Orius 600) was used to capture images in the microscopy department of the intradepartmental unit
490 of Hebrew University.

491 **Acne vulgaris mouse model**

492 For the induction of acne vulgaris lesions, we used the clinically highly virulent *C. acnes* strain
493 S.27 (Sheffer-Levi et al., 2020). Bacteria were grown for three days and brought to a concentration
494 of 10^9 CFU/ml, and 50 μ l of bacteria were injected intradermally into the right and left sides of
495 the back of 34 ICR eight-week-old albino mice, for a total of 68 lesions (Kolar et al., 2019). A
496 second intradermal bacterial infection was performed again after 24 h in the same region, as the
497 lesions were not sufficient after one injection. Based on a previous report showing that synthetic
498 sebum enhances inflammatory acne vulgaris lesions in an acne vulgaris mouse model (Kolar et al.,
499 2019), 20 μ l of artificial sebum (prepared by mixing 17% fatty acid, oleic acid, triolein, 25% jojoba
500 oil, and 13% squalene) was applied immediately, following the first intradermal injection, and
501 reapplied daily for the duration of the experiment. Mice were sacrificed three days post-last gel
502 administration. Chlorhexidine cleaning of the lesion and three days without treatment assured that
503 the phages isolated *ex vivo* were not the phages recently applied and not absorbed. For flow
504 cytometry analysis, 15 mice were sacrificed at three timepoints. Three mice on day three before
505 receiving any treatment. On day five, three phage-treated mice and three control-treated mice were
506 sacrificed; on day seven, three phage-treated mice and three control-treated mice were sacrificed.
507 From several mice, uninfected skin was taken as a negative control.







508 **Topical phage treatment**

509 Mice were randomly assigned to two groups of 17 mice, with each group treated daily for five
510 days. The control group received a topical 2.5% carbopol gel (Super-Pharm, Herzliya, Israel), and
511 the treated group received a 2.5% carbopol gel containing a *C. acnes* phage, FD3, at a concentration
512 of 10^9 PFU/ml. The groups were separated to prevent the transfer of phages between them.

513 **Assessment of phage clinical efficacy**

514 Photography was performed daily. The degree of clinical inflammatory changes was recorded
515 daily using three clinical parameters: 1) measurement of the lesion diameter using an electronic
516 caliper (Winstar), 2) degree of elevation/papulation of inflammatory lesions, and 3) presence and
517 severity of eschar within inflammatory lesions. A clinical scoring system was developed and
518 evaluated (Figure 7) by combining the three abovementioned clinical parameters. The scoring
519 system was developed based on various clinical acne vulgaris scoring methods (Agnew et al.,

520 2016; Qin et al., 2015), including the revised acne Leeds grading system (O’Brien et al., 1998). To
 521 avoid bias, the score was evaluated blindly by two independent investigators. The unit of the score
 522 was AU. The eschar score was corrected to the same initial score because of uneven mouse
 523 allocation of this clinical parameter.

Characteristic	Value	Score (AU)	Example
Diameter	0-1.9 mm	0	
	2-3.9 mm	1	
	4-5.9 mm	2	
	6-8 mm = 3	3	
Elevation (Double Blinded)	Flat	0	
	Small	1	
	Large	2	
Eschar (Double Blinded)	No	0	
	Mild	1	
	Marked	2	

524
 525 **Figure 7. Definition of the clinical scoring of mice.**
 526 The following parameters were used to score the severity of the lesions based on a modified revised
 527 acne Leeds grading system (O’Brien et al., 1998) and other methods previously described for the
 528 clinical scoring of acne vulgaris (Agnew et al., 2016; Qin et al., 2015). The total score, with a

529 range of 0–7, was calculated by summing up the parameters. Refer to the assessment of phage
530 clinical efficacy subsection in the Materials and Methods section for more details.

531

532

533

534

535 **Histopathological evaluation**

536 Punch skin biopsies of 3 mm were obtained from inflammatory lesions at the end of the treatment.
537 Several representative biopsies were used for histopathological evaluation, and the other tissue
538 samples were homogenized in sterile phosphate buffered saline (PBS) using stainless steel beads
539 and a bullet blender tissue homogenizer (Next Advance) for bacterial and phage assays. The
540 presence of bacteria at the lesion's site was validated by PCR using the following specific primers:
541 the SLST primer, forward primer 5'-CAGCGGCGCTGCTAAGAACTT-3', and reverse primer
542 5'-CCGGCTGGCAAATGAGGCAT-3'. The presence of the phage was assessed using the
543 specific forward primers 5'TGATGCTGTAGGTGGCTGTG-3' and reverse primer 5'-
544 CCGAGACGAAATGACCACCA-3'. For phage recognition, a CFU count was performed for a
545 quantitative assessment of viable bacteria on selective media supplemented with furazolidone
546 (0.5 µg/mL) to inhibit the growth of staphylococci and live phages using a PFU count on the *C.*
547 *acnes* bacterial lawn.

548 Pathological skin evaluation of *C. acnes*-injected lesions was performed using tissue biopsies
549 soaked in formalin for fixation, trimmed, embedded in paraffin, and sectioned, followed by
550 staining with hematoxylin and eosin. The histological processing of the biopsies, including
551 embedding, sectioning of tissues, and preparation of slides, was performed in the Histology
552 Laboratory of the Animal Facilities of the Faculty of Medicine of Hebrew University.

553 **Flow cytometry**

554 Extraction of immune cells from skin biopsies was performed using the protocol of Lou *et al.* (Lou
555 *et al.*, 2020), with some modifications to the Dispase II concentration and incubation time. Briefly,
556 1 cm × 1 cm of skin was taken from the inflammatory lesions of sacrificed mice. The skin was
557 washed in Hanks' Balanced Salt Solution (HBSS) three times, cut into four pieces diagonally, and
558 incubated with 8 mg/ml Dispase II (Merck, Kenilworth, New Jersey) for 12 h. Following dermis
559 and epidermis separation, the dermis was cut and put in 3.5 ml of Dermis Dissociation Buffer

560 composed of 100 µg/mL of DNASE I (Merck) and 1 mg/ml collagenase P (Merck, Kenilworth
561 New Jersey) in Dulbecco's Modified Eagle Medium (DMEM/high glucose) (Merck, Kenilworth
562 New Jersey, USA) for 1 h. Suspensions were passed through a 40-µm strainer into a 50 ml tube
563 and rinsed again in 12 ml of DMEM with 10% Fetal bovine serum (FBS) (Merck, Kenilworth New
564 Jersey) in 15 ml tubes, centrifuged at 400 g for 5 min at 4°C, supplied with 2 ml of staining buffer
565 (Lou et al., 2020) composed of PBS with 2% Fetal calf serum (FBS (Merck, Kenilworth, New
566 Jersey, USA), and fixated with 250 µl BD Cytotfix™ (BD Biosciences, Franklin Lakes, New
567 Jersey, USA).

568 Single-cell suspensions were incubated and labeled with the following antibodies obtained from
569 BioLegend (San Diego, CA, USA) at a 1:100 dilution: CD115 (AFS98), CD45 (30-f11), CD64
570 (X54-5/7.1), CD11b (M1/70), LY6C (HK1.4), LY6G (1A8), and Zombie UV™ for dead cell
571 exclusion. Following membrane staining, the cells were fixed using a Fixation/Permeabilization
572 Solution Kit (BD) according to the manufacturer's instructions. Flow cytometry was performed
573 using Cytex® Aurora (Cytex, Fremont, CA, USA), and data were analyzed offline using FlowJo
574 10.7.2 (BD Biosciences, Franklin Lakes, New Jersey, USA).

575

576 **Statistical analysis**

577 GraphPad Prism 8.0.2 (42) was used to perform the statistical analysis and graph formation.
578 Significance was calculated using the Student's t-test two-tailed unpaired *p-values* and the Mann–
579 Whitney U-test (significance level: $p < 0.05$). Pearson *r* and *r* square regression models were used.
580 The results were the mean of at least three independent experiments.

581

582 **Study approval**

583 This study was approved by the Authority for Biological and Biomedical Models at our institution
584 (Approval number: MD1815519\3).

585

586 **References and Notes**

- 587 Abedon, S.T. (2009). Phage evolution and ecology. *Adv. Appl. Microbiol.* 67, 1–45.
588 Adams, M.H. (1959). *Bacteriophages*. (New York: Interscience Publishers).
589 Agnew, T., Furber, G., Leach, M., and Segal, L. (2016). A comprehensive critique and review of
590 published measures of acne severity. *J. Clin. Aesthet. Dermatol.* 9, 40.

- 591 Barnard, E., Shi, B., Kang, D., Craft, N., and Li, H. (2016). The balance of metagenomic
592 elements shapes the skin microbiome in acne and health. *Sci. Rep.* *6*, 1–12.
- 593 Van Belleghem, J.D., Dąbrowska, K., Vaneechoutte, M., Barr, J.J., and Bollyky, P.L. (2019).
594 Interactions between Bacteriophage, Bacteria, and the Mammalian Immune System. *Viruses* *11*.
- 595 Brüggemann, H., and Lood, R. (2013). Bacteriophages infecting *Propionibacterium acnes*.
596 *Biomed Res. Int.* *2013*.
- 597 BRZIN, B. (1964). Studies on the *Corynebacterium acnes*. *Acta Pathol. Microbiol. Scand.* *60*,
598 599–608.
- 599 Castillo, D.E., Nanda, S., and Keri, J.E. (2019). *Propionibacterium* (*Cutibacterium*) *acnes*
600 bacteriophage therapy in acne: Current evidence and future perspectives. *Dermatol. Ther.*
601 (Heidelb). *9*, 19–31.
- 602 Cheng, L., Marinelli, L.J., Grosset, N., Fitz-Gibbon, S.T., Bowman, C.A., Dang, B.Q., Russell,
603 D.A., Jacobs-Sera, D., Shi, B., Pellegrini, M., et al. (2018). Complete genomic sequences of
604 *Propionibacterium freudenreichii* phages from Swiss cheese reveal greater diversity than
605 *Cutibacterium* (formerly *Propionibacterium*) *acnes* phages. *BMC Microbiol.* *18*, 19.
- 606 Coates, P., Vyakrnam, S., Eady, E.A., Jones, C.E., Cove, J.H., and Cunliffe, W.J. (2002).
607 Prevalence of antibiotic-resistant propionibacteria on the skin of acne patients: 10-year
608 surveillance data and snapshot distribution study. *Br. J. Dermatol.* *146*, 840–848.
- 609 Dessinioti, C., and Katsambas, A.D. (2010). The role of *Propionibacterium acnes* in acne
610 pathogenesis: facts and controversies. *Clin. Dermatol.* *28*, 2–7.
- 611 Genel, F., Atlihan, F., Gulez, N., Kazanci, E., Vergin, C., Terek, D.T., and Yurdun, O.C. (2012).
612 Evaluation of adhesion molecules CD64, CD11b and CD62L in neutrophils and monocytes of
613 peripheral blood for early diagnosis of neonatal infection. *World J. Pediatr.* *8*, 72–75.
- 614 Jassim, S.A.A., and Limoges, R.G. (2014). Natural solution to antibiotic resistance:
615 bacteriophages ‘The Living Drugs.’ *World J. Microbiol. Biotechnol.* *30*, 2153–2170.
- 616 Jong, E.C., Ko, H.L., and Pulverer, G. (1975). Studies on bacteriophages of *Propionibacterium*
617 *acnes*. *Med. Microbiol. Immunol.* *161*, 263–271.
- 618 Karadag, A.S., Aslan Kayıran, M., Wu, C., Chen, W., and Parish, L.C. (2020). Antibiotic
619 resistance in acne: changes, consequences and concerns. *J. Eur. Acad. Dermatology Venereol.*
- 620 Katsambas, A.D., Stefanaki, C., and Cunliffe, W.J. (2004). Guidelines for treating acne. *Clin.*
621 *Dermatol.* *22*, 439–444.
- 622 Kim, J., Ochoa, M.-T., Krutzik, S.R., Takeuchi, O., Uematsu, S., Legaspi, A.J., Brightbill, H.D.,
623 Holland, D., Cunliffe, W.J., and Akira, S. (2002). Activation of toll-like receptor 2 in acne
624 triggers inflammatory cytokine responses. *J. Immunol.* *169*, 1535–1541.
- 625 Kim, M.J., Eun, D.H., Kim, S.M., Kim, J., and Lee, W.J. (2019). Efficacy of bacteriophages in
626 *Propionibacterium acnes*-induced inflammation in mice. *Ann. Dermatol.* *31*, 22–28.
- 627 Kolar, S.L., Tsai, C.-M., Torres, J., Fan, X., Li, H., and Liu, G.Y. (2019). *Propionibacterium*
628 *acnes*-induced immunopathology correlates with health and disease association. *JCI Insight* *4*.
- 629 Lam, H.Y.P., Lai, M.-J., Chen, T.-Y., Wu, W.-J., Peng, S.-Y., and Chang, K.-C. (2021).
630 Therapeutic Effect of a Newly Isolated Lytic Bacteriophage against Multi-Drug-Resistant

- 631 Cutibacterium acnes Infection in Mice. *Int. J. Mol. Sci.* 22, 7031.
- 632 Li, Z.J., Choi, D.K., Sohn, K.C., Seo, M.S., Lee, H.E., Lee, Y., Seo, Y.J., Lee, Y.H., Shi, G., and
633 Zouboulis, C.C. (2014). Propionibacterium acnes activates the NLRP3 inflammasome in human
634 sebocytes. *J. Invest. Dermatol.* 134, 2747–2756.
- 635 Liu, J., Yan, R., Zhong, Q., Ngo, S., Bangayan, N.J., Nguyen, L., Lui, T., Liu, M., Erfe, M.C.,
636 Craft, N., et al. (2015). The diversity and host interactions of Propionibacterium acnes
637 bacteriophages on human skin. *ISME J.* 9, 2078–2093.
- 638 Lomholt, H.B., and Kilian, M. (2010). Population genetic analysis of Propionibacterium acnes
639 identifies a subpopulation and epidemic clones associated with acne. *PLoS One* 5, e12277.
- 640 Lou, F., Sun, Y., and Wang, H. (2020). Protocol for Flow Cytometric Detection of Immune Cell
641 Infiltration in the Epidermis and Dermis of a Psoriasis Mouse Model. *STAR Protoc.* 100115.
- 642 Marinelli, L.J., Fitz-Gibbon, S., Hayes, C., Bowman, C., Inkeles, M., Loncaric, A., Russell,
643 D.A., Jacobs-Sera, D., Cokus, S., and Pellegrini, M. (2012). Propionibacterium acnes
644 bacteriophages display limited genetic diversity and broad killing activity against bacterial skin
645 isolates. *MBio* 3.
- 646 Muhammad, M., and Rosen, T. (2013). A controversial proposal: no more antibiotics for acne.
647 *Ski. Ther. Lett* 18, 1–4.
- 648 Nelson, D.C., Schmelcher, M., Rodriguez-Rubio, L., Klumpp, J., Pritchard, D.G., Dong, S., and
649 Donovan, D.M. (2012). Chapter 7 - Endolysins as Antimicrobials. In *Bacteriophages, Part B*, M.
650 Łobocka, and W.B.T.-A. in V.R. Szybalski, eds. (Academic Press), pp. 299–365.
- 651 O’Brien, S., Lewis, J., and Cunliffe, W. (1998). The Leeds revised acne grading system. *J.*
652 *Dermatolog. Treat.* 9, 215–220.
- 653 O’Neill, A.M., and Gallo, R.L. (2018). Host-microbiome interactions and recent progress into
654 understanding the biology of acne vulgaris. *Microbiome* 6, 177.
- 655 Plewig, G., Melnik, B., and Chen, W. (2019). Acne Research Models BT - Plewig and
656 Kligman’s Acne and Rosacea. G. Plewig, B. Melnik, and W. Chen, eds. (Cham: Springer
657 International Publishing), pp. 595–608.
- 658 Qin, X., Li, H., Jian, X., and Yu, B. (2015). Evaluation of the efficacy and safety of fractional
659 bipolar radiofrequency with high-energy strategy for treatment of acne scars in Chinese. *J.*
660 *Cosmet. Laser Ther.* 17, 237–245.
- 661 Rzany, B., and Kahl, C. (2006). Epidemiology of acne vulgaris. *J. Der Dtsch. Dermatologischen*
662 *Gesellschaft= J. Ger. Soc. Dermatology JDDG* 4, 8–9.
- 663 Sheffer-Levi, S., Rimon, A., Lerer, V., Shlomov, T., Copenhagen-Glazer, S., Rakov, C., Zeiter,
664 T., Nir-Paz, R., Hazan, R., and Molcho-Pessach, V. (2020). Antibiotic Susceptibility of
665 Cutibacterium acnes Strains Isolated from Israeli Acne Patients. *Acta Derm. Venereol.*
- 666 Summer, E.J. (2009). Preparation of a phage DNA fragment library for whole genome shotgun
667 sequencing. In *Bacteriophages*, (Springer), pp. 27–46.
- 668 Swamydas, M., Luo, Y., Dorf, M.E., and Lionakis, M.S. (2015). Isolation of mouse neutrophils.
669 *Curr. Protoc. Immunol.* 110, 3–20.
- 670 Swanson, J.K. (2003). Antibiotic resistance of Propionibacterium acnes in acne vulgaris.

- 671 Dermatology Nurs. *15*, 359–363.
- 672 Thierry, A., Deutsch, S.-M., Falentin, H., Dalmasso, M., Cousin, F.J., and Jan, G. (2011). New
673 insights into physiology and metabolism of *Propionibacterium freudenreichii*. *Int. J. Food*
674 *Microbiol.* *149*, 19–27.
- 675 Toyne, H., Webber, C., Collignon, P., Dwan, K., and Kljakovic, M. (2012). *Propionibacterium*
676 *acnes* (P. *acnes*) resistance and antibiotic use in patients attending Australian general practice.
677 *Australas. J. Dermatol.* *53*, 106–111.
- 678 Wayne, P.A. (2017). Performance Standards for Antimicrobial Susceptibility Testing: Twenty-
679 Seventh Informational Supplement M100-S27. Wayne, PA CLSI.
- 680 Yazdi, M., Bouzari, M., Ghaemi, E.A., and Shahin, K. (2020). Isolation, Characterization and
681 Genomic Analysis of a Novel Bacteriophage VB_EcoS-Golestan Infecting Multidrug-Resistant
682 *Escherichia coli* Isolated from Urinary Tract Infection. *Sci. Rep.* *10*, 7690.
- 683 Yerushalmy, O., Khalifa, L., Gold, N., Rakov, C., Alkalay-Oren, S., Adler, K., Ben-Porat, S.,
684 Kraitman, R., Gronovich, N., and Shulamit Ginat, K. (2020). The Israeli Phage Bank (IPB).
685 *Antibiotics* *9*, 269.
- 686 Zaenglein, A.L. (2018). Acne vulgaris. *N. Engl. J. Med.* *379*, 1343–1352.
- 687 Zaenglein, A.L., Pathy, A.L., Schlosser, B.J., Alikhan, A., Baldwin, H.E., Berson, D.S., Bowe,
688 W.P., Graber, E.M., Harper, J.C., and Kang, S. (2016). Guidelines of care for the management of
689 acne vulgaris. *J. Am. Acad. Dermatol.* *74*, 945–973.

690

691 **Acknowledgments:** We would like to thank Simon Yona for advising with flow cytometry, and
692 suppling the materials for flow analysis. We would also like to thank the Core Research
693 Facility of Hebrew University, Ein Karem Campus, Abed Nasereddin and Idit Shiff for
694 the deep sequencing, and Eduardo Berenshtein for the TEM.
695 We are grateful to Mariana Scherem for helping us prepare our *in vivo* experiments.

696 **Funding:**

697 United States–Israel Binational Science Foundation Grant #2017123
698 Israel Science Foundation IPMP Grant #ISF1349/20
699 Rosetrees Trust Grant A2232
700 Milgrom Family Support Program
701 Gishur Fund of Hadassah Medical Center
702 George and Linda Hiltzick’s donation to Hadassah Medical Center

703 **Authors’ contributions:**

704 **Conceptualization:** AR, CR, VMP, RH
705 **Methodology:** AR, CR, SCG, VMP RH
706 **Experiment and analysis:** AR, CR, VL, SSL, SAO, TS, LS, RL
707 **Funding:** VMP, RH
708 **Project administration:** SCG, VMP, RH
709 **Supervision:** SCG, VMP, RH
710 **Writing (original draft):** AR, CR, SAO, VMP, RH

711 **Writing (review and editing):** SCG

712 **Competing interests:** The authors declare that they have no competing interests.

713 **Data and materials availability:** All data, codes, and materials used in the analysis must be
714 available in some form to any researcher for the purpose of reproducing or extending the
715 analysis. Include a note explaining any restrictions on materials, such as material transfer
716 agreements (MTAs). Note accession numbers to any data related to the paper and
717 deposited in a public database; include a brief description of the data set or model with
718 the number. If all data are in the paper and supplementary materials, include the sentence,
719 “All data are available in the main text or the supplementary materials.”
720